



COMMUNICATION

Molecular Determinants of Self-Association and Rearrangement of a Trimeric Intermediate during the Assembly of a Parvovirus Capsid

Rebeca Pérez, Milagros Castellanos, Alicia Rodríguez-Huete and Mauricio G. Mateu*

Centro de Biología Molecular "Severo Ochoa" (Consejo Superior de Investigaciones Científicas-Universidad Autónoma de Madrid), Cantoblanco, 28049 Madrid, Spain

Received 12 May 2011;
received in revised form
26 July 2011;
accepted 9 August 2011
Available online
16 August 2011

Edited by M. Moody

Keywords:

supramolecular complex;
virus morphogenesis;
molecular recognition;
protein–protein interactions;
structure–function analysis

The minute virus of mice (MVM) provides a simple model for the dissection of the molecular determinants of the self-assembly, stability, and dynamics of a biological supramolecular complex. MVM assembly involves the trimerization of capsid subunits in the cytoplasm; trimers are transported to the nucleus, where they suffer a conformational change and are made competent for capsid formation. Our previous study revealed that capsid assembly from trimers is dependent on stronger intertrimer interactions that are equally spaced in an equatorial belt surrounding each trimer. We have now targeted the interfaces between monomers within each trimer to identify the molecular determinants of trimerization and the rearrangement needed for capsid assembly. Twenty-eight amino acid residues per monomer were individually mutated to alanine to remove most of the stronger intersubunit interactions. The effects on trimer and capsid assembly and virus infectivity in cells were analyzed. No side chain was individually required for trimer assembly in the cytoplasm; in contrast, half of them were required to make the trimers competent for nuclear capsid assembly, even though none was close to intertrimer interfaces. These critical side chains are conserved and participate in extensive hydrophobic contacts, buried hydrogen bonds, or salt bridges between subunits. This study on MVM capsid assembly reveals that: (i) trimerization is a robust process, insensitive to removal of individual intersubunit interactions; and (ii) the rearrangement of the trimer intermediate required for capsid assembly is a global process that depends on the establishment of many interactions along the protein–protein interfaces within each trimer.

© 2011 Elsevier Ltd. All rights reserved.

The study of macromolecular self-assembly is critical for a molecular understanding of many biological functions and the engineering of self-organizing nanodevices.^{1–7} Alanine scanning

mutagenesis⁸ has been undertaken for many small protein–ligand complexes or oligomeric proteins to identify the individual roles of amino acid residues, and interactions between subunits, in protein–protein recognition.^{9,10} However, only a few such studies are available for large ensembles such as virus capsids^{11–18} or capsid-like proteins.¹⁹ We have chosen a parvovirus,²⁰ the minute virus of mice (MVM),²¹ as a minimalist model for a systematic study of the molecular determinants of self-assembly in virus capsids.

*Corresponding author. E-mail address: mgarcia@cbm.uam.es.

Abbreviations used: MVM, minute virus of mice; VP, viral protein; MVMp, MVM strain p; mAb, monoclonal antibody.

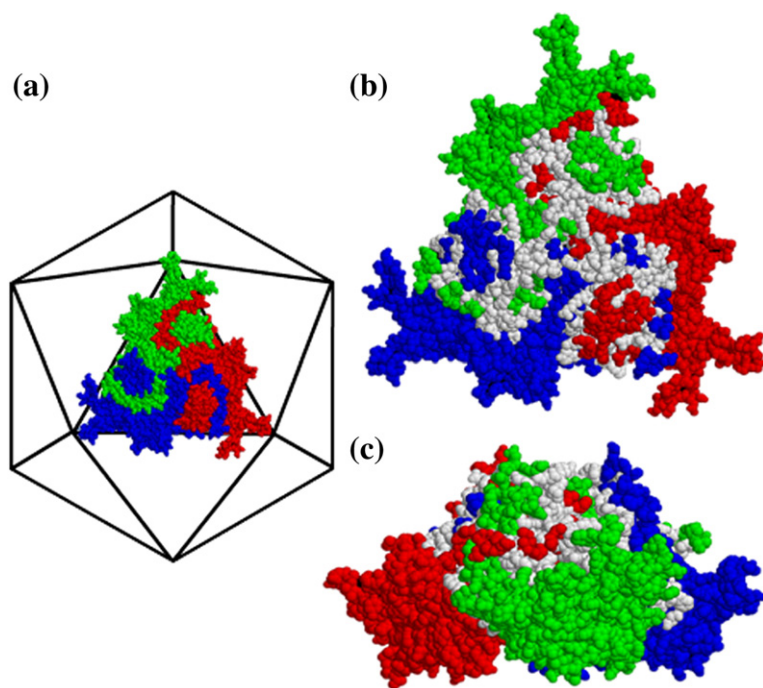


Fig. 1. Structure of the MVM capsid. (a) Schematic representation of the icosahedral ($T=1$ MVM) capsid. A trimer is represented as a space-filling model, with its three subunits shown in green, red, and blue. (b) Front view of a trimer. (c) Lateral view of a trimer. The residues of the three subunits involved in intersubunit interactions within the trimer are shown in white.

The icosahedral MVM capsid (Fig. 1a), as in other parvoviruses,²² is assembled from 60 equivalent subunits contributed by viral proteins (VP) VP1 and VP2, which show identical fold and core sequences and differ just by an N-terminal extension in VP1.^{23,24} Intersubunit interactions involve residues and structural elements shared by all subunits; the disordered N-termini of VP1 and VP2 do not contribute to self-assembly.^{24,25}

Trimers of VPs (Fig. 1) act as capsid assembly intermediates in MVM.^{22,26–30} The VP polypeptides in each trimer are intertwined through long surface loops, forming convoluted intratrimer interfaces (Fig. 1b and c); the trimers are more loosely connected between them through quasi-linear interfaces. In the cytoplasm, VPs of MVM fold and associate to form trimers that are incompetent for capsid assembly. Trimers (but not individual VPs) translocate to the nucleus, where they are made competent for intertrimer association to form the viral capsid, thus providing a morphogenetic control step.²⁷ This step involves a global conformational rearrangement of the trimer that was revealed by the capsid-assembly-dependent generation of a conformation-dependent epitope on top of a protrusion (spike) at the center of each trimer.^{27,31,32}

In a previous study, we found that MVM capsid assembly from trimers is dependent on a few stronger hydrophobic contacts or buried electrostatic interactions between trimers that are equally spaced in an equatorial belt surrounding each trimer.¹⁷ In the present study, we have investigated the molecular determinants of the previous trimerization reaction and of the conformational rearrangement of the trimer.

Analysis of interactions between monomers in an MVM capsid trimer and selection of residues for mutational analysis

The residues and interactions at the interfaces between monomers within each trimer (Fig. 1b and c) are essentially conserved between the empty capsid and the virion.^{23,24} Analysis of the refined crystal structure of the MVM strain p (MVMp) capsid²⁴ indicated that 170 of the 587 amino acid residues per monomer (VP2) are involved in intermonomer interactions in each trimer. The intertrimer and intratrimer interfaces are essentially nonoverlapping; only one residue (N544) participates in both interfaces through a substantial number of interprotein contacts.

For 120 residues at the intratrimer interfaces, side-chain atoms beyond C^β participate in intermonomer interactions; most of the remaining 50 residues are involved in interactions with the side chain (beyond C^β) of a partner residue in the neighboring monomer. Based on thermodynamic considerations and our study of MVM intertrimer interfaces,¹⁷ we have classified into two groups the side chains at the intermonomer interfaces within each trimer (Table S1). Group S includes 46 side chains (per monomer) that are presumably involved in potentially stronger interactions, including a substantial number of hydrophobic contacts and/or hydrogen bonds or salt bridges essentially buried within the interfaces. Group W includes 74 side chains that would establish only weaker interactions. About 50% of the residues in group S are conserved in six or all seven parvoviruses compared, while only

about 30% of the residues in group W are similarly conserved.³³

Based on the above analysis, we chose for mutation a large number of group S residues that could potentially make major contributions towards holding three monomers together in each trimer. We favored those residues that are highly conserved, the ones whose side chain (beyond C^β) established fewer intramonomer contacts, and those that established no intertrimer contacts. In this manner, any

observed effect of the mutations could be reasonably attributed to the removal of intermonomer—not intramonomer or intertrimer—interactions.

In all, 24 group S residues were chosen (Table 1). Because mutation of only one residue of any one pair involved in an interaction would be enough to eliminate that interaction, mutation to alanine of those 24 residues would together disrupt a very high proportion of the intermonomer interactions in each trimer (20 of the 21 buried hydrogen bonds, all 6

Table 1. Effect of the truncation of intratrimer side chains on trimer and capsid assembly and virus infectivity

Mutant	Group ^a	Conservation of each residue ^b	Intersubunit interactions within a trimer			Assembled capsids (C/V ratio ^c)	Normalized virus titer ^d
			Salt bridges ^e	Hydrogen bonds ^f	Van der Waals (C–C) ^g		
wt						1	1
Y214A	S	C	—	1 E327, 1 R330, 2 R332	42 (25)	ND	NO
W283A	S	C	—	—	32 (16)	0.08	NO
R287A	S	C	1 D101	—	21 (3)	0	NO
R314A	S	C	2 D102	—	2 (0)	0	NO
Q319A	S	C	—	2 K357, 1 G372	10 (1)	0	NO
W324A	S	—	—	—	20 (17)	0	NO
S326A	S	—	—	1 D101	2 (0)	0.2	NO
S348A	S	—	—	1 G406	1 (0)	0.05	NO
F413A	S	—	—	—	17 (17)	0	NO
N448A	S	C	—	1 N448, 1 Y450	2 (0)	0.05	NO
Y450A	S	C	—	—	13 (11)	0	NO
D470A	S	C	—	1 Y587	2 (0)	0	NO
L475A	S	—	—	—	7 (5)	0	NO
N544A	S	C	—	1 S245	1 (0)	0.03	NO
V86A	S	C	—	—	6 (5)	0.42	3.5 × 10 ^{−4}
K100A	S	—	—	—	14 (12)	1.06	1.3 × 10 ^{−1}
W108A	S	—	—	—	8 (8)	0.89	4.3 × 10 ^{−1}
Q291A	S	—	—	1 S194, 1 S209	12 (4)	0.73	5.5 × 10 ^{−4}
E346A	S	C	2 R407	1 Q335, 1 S449	6 (1)	1.05	6.2 × 10 ^{−2}
R349A	S	—	1 D361	—	16 (5)	0.8	4.3 × 10 ^{−1}
L453A	S	C	—	—	5 (5)	0.95	6.5 × 10 ^{−3}
H458A	S	—	—	1 H477	3 (0)	0.63	4 × 10 ^{−1}
H477A	S	—	—	1 H458, 2 R480	11 (5)	0.97	1.9 × 10 ^{−2}
R584A	S	—	1 D474	—	3 (0)	0.61	ND
V374A	W	—	—	—	1 (0)	0.69	2.2 × 10 ^{−3}
Q311A	W	—	—	1 K100	7 (0)	1.08	2 × 10 ^{−2}
L419A	W	—	—	—	1 (0)	0.74	1.7 × 10 ^{−2}
I483A	W	—	—	—	1 (1)	1.26	1.2 × 10 ^{−1}

ND, not determined.

^a Group S includes residues that are involved in presumably stronger intersubunit interactions within a trimer [buried hydrogen bonds and/or salt bridges and/or five or more hydrophobic (C–C) contacts]. Group W includes residues that are involved in presumably weaker interactions (no buried hydrogen bonds or salt bridges, and less than five C–C contacts).

^b C: the same residue was found in at least six of the seven parvoviruses compared.³³

^c Determined by *in situ* immunofluorescence assays. The C/V ratio was obtained by dividing the number of cells that were positive for capsid assembly (C) by the number of cells that were positive for VP expression (V).³⁵

^d The mutations were introduced by subcloning^{27,37,53} in an MVMP infectious clone⁵⁴ originally provided by P. Tattersall (Yale University Medical School, New Haven, CT) and modified.⁵² The concentration of purified DNA was estimated by agarose gel electrophoresis and ethidium bromide staining, and/or quantitated using a Nanodrop spectrophotometer. NB324K cells were electroporated^{28,29} and incubated for 4 days, and the viral progeny titers were determined in two to five independent plaque assay experiments. Each titer was normalized relative to that obtained with the nonmutated infectious plasmid and averaged. NO, the mutant, was not titrated as it was unable to yield detectable amounts of capsid and thus was essentially noninfectious. Control experiments with several mutants for which the amount of VPs expressed and present in the transfected cells was quantitated in immunoassays revealed that the difference in VP expression was confined to within half and double of that obtained with the control. Thus, we consider as significant any difference in viral titer that is equal to or greater than one order of magnitude.

^e The residues involved in intersubunit salt bridges with each mutated residue are indicated. All salt bridges, except for R349-D361, are essentially buried.

^f The residues involved in intersubunit hydrogen bonds with each mutated residue are indicated. All hydrogen bonds, except for Q311-K100, are essentially buried.

^g The number of intersubunit van der Waals contacts and (in parentheses) those of them that involve C–C contacts with the side chain (beyond C^β) of each mutated residue are indicated.

buried salt bridges, and 12 of the 17 major clusters of hydrophobic contacts per monomer). Partly as a control, 4 group W residues were also included in the analysis (Table 1). The effect of each mutation on the different stages of capsid assembly and virus infectivity was analyzed.

Role of residues at the intratrimer interfaces in trimer assembly in mammalian cells

Cells were transformed with recombinant plasmids that code for mutant capsid proteins, and VP expression, folding and trimerization, and capsid

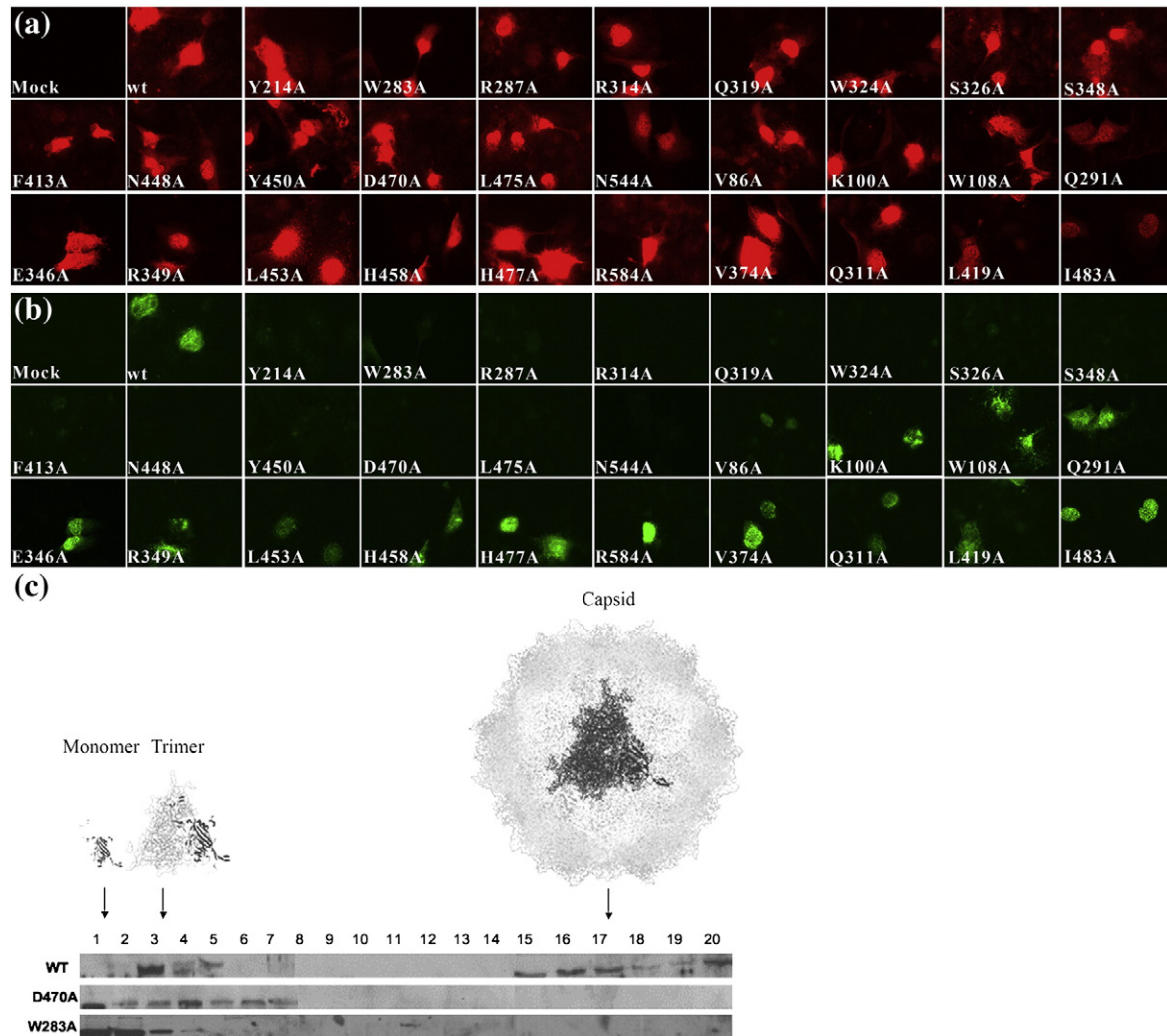


Fig. 2. Effect on trimer and capsid assembly of the mutation to Ala of residues involved in intersubunit interactions within a trimer. (a and b) *In situ* immunofluorescence analysis. Mammalian NB324K cells were electroporated^{28,29} with the pSVtk-VP1/2 plasmid (which contains the VP1/VP2 gene of MVMp⁵² carrying the mutation indicated in each figure), incubated for 2 days, and analyzed in *in situ* immunofluorescence assays.^{27–29} Equal nonsaturating amounts of plasmids carrying the chosen mutations and the corresponding nonmutated plasmid used as a positive control were included in each experiment. (a) Positive assembly of trimers was ascertained by the presence of nuclear fluorescence using a polyclonal antibody that recognizes VPs of MVM.²⁷ (b) Positive assembly of capsids was ascertained by the presence of nuclear fluorescence using the capsid-specific mAb B7.³¹ Mock, negative control (no pSVtk-VP1/2 plasmid added); wt, positive control using the nonmutated pSVtk-VP1/2 plasmid. Representative experiments are shown. (c) Sedimentation analysis.²⁷ Cells were transfected with nonmutated (wt) or mutant D470A or W283A pSVtk-VP1/2 plasmid. The MVM particles present in the cell extracts were analyzed by centrifugation in sucrose gradients. The presence of VPs in each fraction was detected by SDS-PAGE and immunoblotting using an anti-VP polyclonal antibody. The approximate positions corresponding to monomeric VP, the trimeric assembly intermediate, and the assembled empty capsid are indicated by arrows. Six other mutants (R314A, R287A, Q319A, S348A, L475A, and N544A) that were also able to assemble into trimers, but not capsids, according to immunofluorescence results were also subjected to sedimentation analysis and yielded a profile equivalent to that shown here for D470A or W283A.

assembly within the cells were analyzed using *in situ* immunofluorescence assays²⁷ (Fig. 2). When an anti-VP antibody was used as a probe, the non-mutated control and all 28 alanine mutants tested reproducibly yielded positive signals of similar intensity (estimated from signals averaged from a sample of cells), indicating that they accumulated similar levels of capsid protein subunits (Fig. 2a). Surprisingly, none of those 28 mutations prevented the normal translocation of the VP subunits to the cell nucleus, as deduced from the normal nuclear fluorescence signal that was reproducibly observed (Fig. 2a).

Trimers, but not individual VPs, are competent for nuclear translocation because this process requires the folding of a nuclear localization motif during trimer association.^{26,27,29,30} Thus, the immunofluorescence results indicated that all 28 mutant VPs are not only expressed but also able to self-associate to form the trimeric intermediate. It could be argued that some mutations could allow nuclear transportation of VPs without a need for trimer assembly. We find it highly unlikely that different stereochemically diverse mutations of widely scattered residues buried in the VP hydrophobic core could have each created an alternative signal to allow VP translocation without the formation of the trimer and the nuclear localization motif. However, to confirm by an independent method that some mutations do not prevent trimer formation, we subjected most of the capsid-assembly-incompetent mutants (8 out of 14) to sedimentation velocity analysis.²⁷ As expected, for the nonmutated control, a certain amount of MVM particles with a sedimentation coefficient corresponding to that of the trimer (about 9S) and a large amount of particles with a sedimentation coefficient corresponding to that of empty capsids (about 70S) were detected (Fig. 2c). Any of the eight tested mutations abolished capsid assembly but did not prevent the accumulation of particles with a sedimentation coefficient similar to that of the trimer (Fig. 2c; data not shown). In a few mutants (W283A in Fig. 2c), a smaller amount of trimers and a larger amount of what appears to correspond to monomers were observed, suggesting that those particular mutations could impair—but not prevent—trimer formation.

One possible explanation for the ability of all tested mutants to form trimers is based on the large number of strong hydrophobic and buried electrostatic interactions at the convoluted intratrimer interfaces, compared to the smaller number of similar interactions at the relatively planar and less extended intertrimer interfaces (or at interfaces in many nonviral oligomeric proteins). Each individual protein–protein interaction within a trimer, however strong, may not contribute a very significant part of the interaction free energy that holds the subunits together, and no critical interaction hot spots may

exist. This is by no means an obvious explanation as, on the other hand, each mutation in the capsid involves the removal of 60 side chains (one per monomer). Even if highly complex protein–protein interfaces are considered, single amino acid substitutions removing as many as 60 particularly strong protein–protein interactions could critically reduce the cooperativity of the multimerization process.

Another nonexclusive possible explanation for the insensitivity of trimer assembly to individual mutations is that the isolated trimers in the cytoplasm may lack many of the intratrimer interactions observed in the assembled capsid. For example, VP association in the cytoplasm could yield a trimeric assembly intermediate with a less compact but not fully folded conformation. This possibility is consistent with the available evidence^{26,27,29,31,32,34} (see also the text below). A direct comparison of the structure of the isolated trimer with that of a trimeric subunit in the capsid is not available yet partly because of the difficulty of isolating trimers in large quantities.

Role of residues at the intratrimer interfaces in trimer–trimer association and capsid assembly in the cell nucleus

To determine the effects of the 28 mutations on the competence for capsid assembly of the trimers transported into the cell nucleus, we used the anti-capsid monoclonal antibody (mAb) B7 in immunofluorescence experiments (Fig. 2b). B7 is not able to recognize trimers that are incompetent for capsid assembly²⁷ but recognizes assembled capsids by specifically binding a conformation-dependent discontinuous epitope located on the center of each trimer.^{31,32} This provides a conformational probe for distinguishing between assembly-incompetent and assembly-competent trimer conformations. As a quantitative measurement of capsid formation, the C/V ratio between the number of cells that were positive for capsid assembly (C) and the number of cells that were positive for VP expression (V)³⁵ was determined for each mutant and normalized (Table 1).

The 4 group W mutants tested were able to assemble into capsids as expected (C/V ratios ≥ 0.7). Ten of the 24 group S mutants tested also yielded normal amounts of capsid (C/V ratios >0.4). Surprisingly, as many as 14 of the 24 group S mutants, while able to translocate to the cell nucleus, were essentially unable to form assembled capsids (C/V ratios <0.05 , in general) (Fig. 2b and Table 1).

If only the immunofluorescence results were taken into account, one could argue that, in fact, mutant capsids could have been normally assembled but that mutation of the interfacial residues could have prevented the binding of the mAb B7. However, this is clearly not the case because all but one of the critical residues are located far away from the B7

epitope; in addition, sedimentation analysis for the majority of these mutants directly showed that they are totally unable to assemble into capsids (Fig. 2c).

The 14 interfacial residues within the trimer that were critical for capsid assembly were mapped on the MVMp structure (Fig. 3). N544 is the only tested residue that is involved also in intertrimer interactions, providing a trivial explanation for the negative effect of the N544A mutation on capsid assembly. The remaining 13 residues are located far away from the intertrimer interfaces and the B7 epitope; nearly all are loosely scattered and completely buried within the trimer. Comparison between the residues critical for assembly and the residues not critical for assembly showed that the former include 83% of the residues at the intratrimer interfaces whose side chain is heavily involved in hydrophobic interactions [11–25 carbon–carbon (C–C) contacts each], 64% of those involved in buried hydrogen bonds or salt bridges between monomers in a trimer, and 62% of those highly conserved in related parvoviruses. In sharp contrast, for the noncritical residues, the above percentages were much lower (16%, 36%, and 21%, respectively).

The simplest interpretation that we found to be consistent with the available evidence is that the critical 13 residues at the monomer–monomer interfaces, located well within each trimer, are needed to facilitate the conformational rearrangement from the capsid-assembly-incompetent trimeric intermediate in the cytoplasm to the assembly-competent trimer in the nucleus.²⁷ As the critical residues are not concentrated in a defined region but scattered over a large area of the protein–protein interfaces within the trimer, the conformational rearrangement may involve a large part of the trimer structure. This observation is consistent with the

evidence mentioned above, which suggests that the cytoplasmic trimer is not in a fully folded conformation. The β -sandwich that forms each VP core may be natively folded, but many of the strong monomer–monomer interactions between the long VP loops would have not been established in the trimer intermediate.³⁴ Translocation into the nucleus or the action of a nuclear factor could lower the energy barrier of the conformational transition to yield a fully folded capsid-assembly-competent trimer. This transition would depend on the establishment of the stronger monomer–monomer hydrophobic contacts and buried electrostatic interactions, thus explaining our observation that most intratrimer mutations that prevent capsid assembly are generally those that remove the stronger interactions. The conformational reorganization of the trimer would modify the relative position of many of the residues at the trimer edges, leading to the generation of stereochemically complementary trimer–trimer surfaces and the acquisition of competence for capsid assembly.

Role of residues at the intratrimer interfaces in MVM infectivity

While half (14) of the mutants analyzed were competent for capsid assembly, their mutation could still cause minor assembly defects and/or affect other steps of the viral cycle. To evaluate this possibility, we individually introduced all but one of these mutations in an MVM infectious clone and transfected mammalian cells for viral progeny analysis. Most (8 out of 13) mutants analyzed showed highly significant reductions in infectivity, with titers that ranged between 4% and 0.1% that of the nonmutated control (Table 1), even in cases

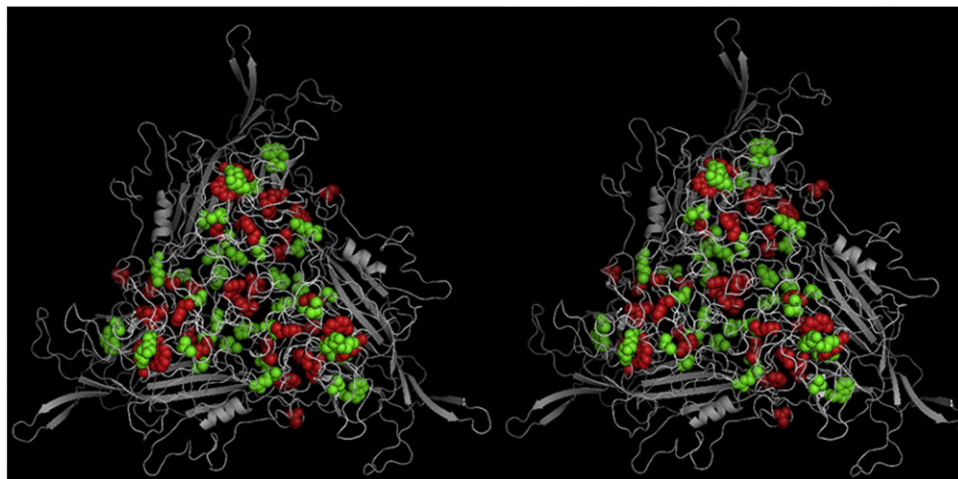


Fig. 3. Mapping of residues at the intersubunit interfaces within a trimer according to their individual requirement for capsid assembly. A stereo view of a trimer (ribbon model) is depicted. The residues at the intratrimer interface whose side chains were found to be critical or dispensable for capsid assembly are, respectively, represented in red or green space-filling models.

where the mutation removed only a few weak interactions. The infectivity results thus revealed a severe functional intolerance to mutation at the intratrimer interfaces in the MVM capsid.

This is by no means an exceptional situation with regard to the capsids of structurally simple viruses. In contrast to that observed for many cellular proteins, multiple structure–function studies reveal that almost every amino acid residue in small nonenveloped virus capsids, including internal and surface residues, may be functionally required for infectivity and/or biological fitness.^{13,17,34,36,37} Small viral capsids appear to have been very finely tuned through evolution because of the many selective constraints imposed on them to fulfill multiple, sometimes conflicting, complex functions with a relatively simple structure. This fine-tuning includes carefully arranged structural overlaps between antigenic regions and receptor binding sites,^{38,39} or special features such as ligand binding in large cavities or covalent modifications during maturation, leading to metastable structures with enough extracellular stability without impairing intracellular dynamics and uncoating of the viral genome.^{40–45}

The MVM capsid, in spite of being one of the structurally simplest known capsids, has been shown to be also subjected to diverse conformational rearrangements, including but not limited to translocation of peptide segments and/or the viral DNA through capsid pores.^{17,21,25–30,34,36,46–50} Many surface and buried residues, including those at inter-trimer interfaces, have been shown through previous mutational analyses to be required for those productive conformational changes and infectivity.¹⁷ Thus, we were not surprised to find that some buried intratrimer interfacial residues that are not critically required for trimer or capsid assembly are, however, needed for normal infectivity. Further studies may show that these functionally critical residues participate in some of the detected conformational transitions of the MVM capsid.

Conclusions

The results obtained complete an unprecedented residue-by-residue analysis of the protein–protein and protein–nucleic acid interfaces involved in the assembly and stability of a virus particle.^{17,36,51} The present study reveals that: (i) none (or very few) of the residues involved in the majority of the presumably stronger protein–protein interactions within each trimeric subunit in the MVM capsid are individually required for the trimerization of capsid proteins in the cytoplasm; trimer self-assembly constitutes a remarkably robust morphogenetic process that may be particularly insensitive to mutation during virus evolution; and (ii) acquisition by the trimeric assembly intermediate of competence for capsid assembly in the cell nucleus involves a global conformational rearrangement that

depends on the establishment of stronger monomer–monomer hydrophobic contacts and buried electrostatic interactions between subunits in the trimer.

Supplementary materials related to this article can be found online at [doi:10.1016/j.jmb.2011.08.020](https://doi.org/10.1016/j.jmb.2011.08.020)

Acknowledgements

Work in the laboratory was supported by grants from the Ministerio de Ciencia y Tecnología (BIO2006-00793 and BIO2009-10092), Comunidad Autónoma de Madrid (S-2009/MAT/1467), and FIPSE (36557/06) to M.G.M., and by an institutional grant from Fundación Ramón Areces. M.G.M. is an associate member of the Center for Biocomputation and Physics of Complex Systems (Zaragoza, Spain). We are indebted to J. M. Almendral and associates for collaboration, continuing advice, technical help and comments, and provision of plasmids and antibodies. We gratefully acknowledge P. Tattersall and C. R. Parrish for originally providing, respectively, the infectious MVMp clone and the mAb B7 obtained through J. M. Almendral, as well as M. A. Fuertes for excellent technical assistance.

References

1. Yeates, T. O. & Padilla, J. E. (2002). Designing supramolecular protein assemblies. *Curr. Opin. Struct. Biol.* **12**, 464–470.
2. Zhang, S. (2003). Fabrication of novel biomaterials through molecular self-assembly. *Nat. Biotechnol.* **21**, 1171–1178.
3. Kentsis, A. & Borden, K. L. (2004). Physical mechanisms and biological significance of supramolecular protein self-assembly. *Curr. Protein Pept. Sci.* **5**, 125–134.
4. Douglas, T. & Young, M. (2006). Host–guest encapsulation of materials by assembled virus protein cages. *Science*, **312**, 873–875.
5. Janin, J., Bahadur, R. P. & Chakrabarti, P. (2008). Protein–protein interaction and quaternary structure. *Q. Rev. Biophys.* **41**, 133–180.
6. Papapostolou, D. & Howorka, S. (2009). Engineering and exploiting protein assemblies in synthetic biology. *Mol. Biosyst.* **5**, 723–732.
7. Mateu, M. G. (2011). Virus engineering: functionalization and stabilization. *Protein Eng. Des. Sel.* **24**, 53–63.
8. Cunningham, B. C. & Wells, J. A. (1989). High-resolution epitope mapping of hGH–receptor interactions by alanine-scanning mutagenesis. *Science*, **244**, 1081–1085.
9. Bogan, A. A. & Thorn, K. S. (1998). Anatomy of hot spots in protein interfaces. *J. Mol. Biol.* **280**, 1–9.
10. Moreira, I. S., Fernandes, P. A. & Ramos, M. J. (2007). Hot spots: a review of the protein–protein interface determinant amino-acid residues. *Proteins*, **68**, 803–812.

11. Wu, P., Xiao, W., Conlon, T., Hughes, J., Agbandje-McKenna, M., Ferkol, T. *et al.* (2000). Mutational analysis of the adeno-associated virus type 2 (AAV2) capsid gene and construction of AAV2 vectors with altered tropism. *J. Virol.* **74**, 8635–8647.
12. Forshey, B. M., von Schwedler, U. K., Sundquist, W. I. & Aiken, C. (2002). Formation of a human immunodeficiency virus type 1 core of optimal stability is crucial for viral replication. *J. Virol.* **76**, 5667–5677.
13. Mateo, R., Diaz, A., Baranowski, E. & Mateu, M. G. (2003). Complete alanine scanning of intersubunit interfaces in a foot-and-mouth disease virus capsid reveals critical contributions of many side chains to particle stability and viral function. *J. Biol. Chem.* **278**, 41019–41027.
14. Del Álamo, M., Neira, J. L. & Mateu, M. G. (2003). Thermodynamic dissection of a low affinity protein–protein interface involved in human immunodeficiency virus assembly. *J. Biol. Chem.* **278**, 27923–27929.
15. Von Schwedler, U. K., Stray, K. M., Garrus, J. E. & Sundquist, W. I. (2003). Functional surfaces of the human immunodeficiency virus type 1 capsid protein. *J. Virol.* **77**, 5439–5450.
16. Ganser-Pornillos, B. K., von Schwedler, U. K., Stray, K. M., Aiken, C. & Sundquist, W. I. (2004). Assembly properties of the human immunodeficiency virus type 1 CA protein. *J. Virol.* **78**, 2545–2552.
17. Reguera, J., Carreira, A., Riobobos, L., Almendral, J. M. & Mateu, M. G. (2004). Role of interfacial amino acid residues in assembly, stability, and conformation of a spherical virus capsid. *Proc. Natl Acad. Sci. USA*, **101**, 2724–2729.
18. Murray, C. L., Jones, C. T., Tassello, J. & Rice, C. M. (2007). Alanine scanning of the hepatitis C virus core protein reveals numerous residues essential for production of infectious virus. *J. Virol.* **81**, 10220–10231.
19. Zhang, Y., Raudah, S., Teo, H., Teo, G. W. S., Fan, R., Sun, X. & Orner, B. P. (2010). Alanine-shaving mutagenesis to determine key interfacial residues governing the assembly of a nano-cage maxi-ferritin. *J. Biol. Chem.* **285**, 12078–12086.
20. Kerr, J., Cotmore, S., Bloom, M. E., Linden, R. M. & Parrish, C. R. (Eds.). (2006). *Parvoviruses*. Hodder Arnold, London, UK.
21. Cotmore, S. F. & Tattersall, P. (2007). Parvoviral host range and cell entry mechanisms. *Adv. Virus Res.* **70**, 183–232.
22. Tsao, J., Chapman, M. S., Agbandje, M., Keller, W., Smith, K., Wu, H. *et al.* (1991). The three-dimensional structure of canine parvovirus and its functional implications. *Science*, **251**, 1456–1464.
23. Agbandje-McKenna, M., Llamas-Saiz, A. L., Wang, F., Tattersall, P. & Rossmann, M. G. (1998). Functional implications of the structure of the murine parvovirus, minute virus of mice. *Structure*, **6**, 1369–1381.
24. Kontou, M., Govindasamy, L., Nam, H. J., Bryant, N., Llamas-Saiz, A. L., Foces-Foces, C. *et al.* (2005). Structural determinants of tissue tropism and *in vivo* pathogenicity for the parvovirus minute virus of mice. *J. Virol.* **79**, 10931–10943.
25. Hernando, E., Llamas-Saiz, A. L., Foces-Foces, C., McKenna, R., Portman, I., Agbandje-McKenna, M. & Almendral, J. M. (2000). Biochemical and physical characterization of parvovirus minute virus of mice virus-like particles. *Virology*, **267**, 299–309.
26. Valle, N., Riobobos, R. & Almendral, J. M. (2006). Synthesis, post-translational modification and trafficking of the parvovirus structural polypeptides. In *Parvoviruses* (Kerr, J. R., Cotmore, S. F., Bloom, M. E., Linden, R. M. & Parrish, C. R., eds), pp. 291–304, Edward Arnold, London, UK.
27. Riobobos, L., Reguera, J., Mateu, M. G. & Almendral, J. M. (2006). Nuclear transport of trimeric assembly intermediates exerts a morphogenetic control on the icosahedral parvovirus capsid. *J. Mol. Biol.* **357**, 1026–1038.
28. Lombardo, E., Ramirez, J. C., Agbandje-McKenna, M. & Almendral, J. M. (2000). A beta-stranded motif drives capsid protein oligomers of the parvovirus minute virus of mice into the nucleus for viral assembly. *J. Virol.* **74**, 3804–3814.
29. Lombardo, E., Ramirez, J. C., Garcia, J. & Almendral, J. M. (2002). Complementary roles of multiple nuclear targeting signals in the capsid proteins of the parvovirus minute virus of mice during assembly and onset of infection. *J. Virol.* **76**, 7049–7059.
30. Maroto, B., Valle, N., Saffrich, R. & Almendral, J. M. (2004). Nuclear export of the nonenveloped parvovirus virion is directed by an unordered protein signal exposed on the capsid surface. *J. Virol.* **78**, 10685–10694.
31. López-Bueno, A., Mateu, M. G. & Almendral, J. M. (2003). High mutant frequency in populations of a DNA virus allows evasion from antibody therapy in an immunodeficient host. *J. Virol.* **77**, 2701–2708.
32. Kaufmann, B., López-Bueno, A., Mateu, M. G., Chipman, P. R., Nelson, C. D., Parrish, C. R. *et al.* (2007). Minute virus of mice, a parvovirus, in complex with the Fab fragment of a neutralizing monoclonal antibody. *J. Virol.* **81**, 9851–9858.
33. Chapman, M. S. & Rossmann, M. G. (1993). Structure, sequence, and function correlations among parvoviruses. *Virology*, **194**, 491–508.
34. Carreira, A., Menendez, M., Reguera, J., Almendral, J. M. & Mateu, M. G. (2004). *In vitro* disassembly of a parvovirus capsid and effect on capsid stability of heterologous peptide insertions in surface loops. *J. Biol. Chem.* **279**, 6517–6525.
35. Grueso, E. (2006). PhD Thesis, Universidad Autónoma de Madrid, Madrid, Spain.
36. Reguera, J., Grueso, E., Carreira, A., Sanchez-Martinez, C., Almendral, J. M. & Mateu, M. G. (2005). Functional relevance of amino acid residues involved in interactions with ordered nucleic acid in a spherical virus. *J. Biol. Chem.* **280**, 17969–17977.
37. Carreira, A. & Mateu, M. G. (2006). Structural tolerance *versus* functional intolerance to mutation of hydrophobic core residues surrounding cavities in a parvovirus capsid. *J. Mol. Biol.* **360**, 1081–1093.
38. Mateu, M. G. (1995). Antibody recognition of picornaviruses and escape from neutralization: a structural view. *Virus Res.* **38**, 1–24.
39. Smith, T. J., Chase, E. S., Schmidt, T. J., Olson, N. H. & Baker, T. S. (1996). Neutralizing antibody to human rhinovirus 14 penetrates the receptor-binding canyon. *Nature*, **383**, 350–354.
40. Rossmann, M. G., Greve, J. M., Kolatkar, P. R., Olson, N. H., Smith, T. J., McKinlay, M. A. & Rueckert, R. R.

- (1997). Rhinovirus attachment and cell entry. In *Structural Biology of Viruses* (Chiu, W., Garcea, R. & Burnette, R., eds), pp. 105–133, Oxford University Press, Oxford, UK.
41. Chow, M., Basavappa, R. & Hogle, J. M. (1997). The role of conformational transitions in poliovirus pathogenesis. In *Structural Biology of Viruses* (Chiu, W., Garcea, R. & Burnette, R., eds), pp. 157–186, Oxford University Press, Oxford, UK.
 42. Hogle, J. M. (2002). Poliovirus cell entry: common structural themes in viral cell entry pathways. *Annu. Rev. Microbiol.* **56**, 677–702.
 43. Johnson, J. E. (2003). Virus particle dynamics. *Adv. Protein Chem.* **64**, 197–218.
 44. Reddy, V. S. & Johnson, J. E. (2005). Structure-derived insights into virus assembly. *Adv. Virus Res.* **64**, 45–68.
 45. Johnson, J. E. (2010). Virus particle maturation: insights into elegantly programmed nanomachines. *Curr. Opin. Struct. Biol.* **20**, 210–216.
 46. Cotmore, S. F., D'Abramo, A. M., Jr., Ticknor, C. M. & Tattersall, P. (1999). Controlled conformational transitions in the MVM virion expose the VP1 N-terminus and viral genome without particle disassembly. *Virology*, **254**, 169–181.
 47. Cotmore, S. F. & Tattersall, P. (2005). Encapsidation of minute virus of mice DNA: aspects of the translocation mechanism revealed by the structure of partially packaged genomes. *Virology*, **336**, 100–112.
 48. Farr, G. A., Cotmore, S. F. & Tattersall, P. (2006). VP2 cleavage and the leucine ring at the base of the fivefold cylinder control pH-dependent externalization of both the VP1 N terminus and the genome of minute virus of mice. *J. Virol.* **80**, 161–171.
 49. Mani, B., Baltzer, C., Valle, N., Almendral, J. M., Kempf, C. & Ros, C. (2006). Low pH-dependent endosomal processing of the incoming parvovirus minute virus of mice virion leads to externalization of the VP1 N-terminal sequence (N-VP1), N-VP2 cleavage, and uncoating of the full-length genome. *J. Virol.* **80**, 1015–1024.
 50. Cotmore, S. F., Hafenstein, S. & Tattersall, P. (2010). Depletion of virion-associated divalent cations induces parvovirus minute virus of mice to eject its genome in a 3'-to-5' direction from an otherwise intact viral particle. *J. Virol.* **84**, 1945–1956.
 51. Carrasco, C., Castellanos, M., de Pablo, P. J. & Mateu, M. G. (2008). Manipulation of the mechanical properties of a virus by protein engineering. *Proc. Natl Acad. Sci. USA*, **105**, 4150–4155.
 52. Ramirez, J. C., Santaren, J. F. & Almendral, J. M. (1995). Transcriptional inhibition of the parvovirus minute virus of mice by constitutive expression of an antisense RNA targeted against the NS-1 transactivator protein. *Virology*, **206**, 57–68.
 53. López-Bueno, A., Rubio, M. P., Bryant, N., McKenna, R., Agbandje-McKenna, M. & Almendral, J. M. (2006). Host-selected amino acid changes at the sialic acid binding pocket of the parvovirus capsid modulate cell binding affinity and determine virulence. *J. Virol.* **80**, 1563–1573.
 54. Gardiner, E. M. & Tattersall, P. (1988). Mapping of the fibrotropic and lymphotropic host range determinants of the parvovirus minute virus of mice. *J. Virol.* **62**, 2605–2613.
 55. Vriend, G. (1990). WHAT IF: a molecular modeling and drug design program. *J. Mol. Graphics*, **8**, 52–56.